Taylor & Francis
Taylor & Francis Group

Journal of Maps

ISSN: 1744-5647 (Online) Journal homepage: www.tandfonline.com/journals/tjom20

Integrated terrestrial and submarine geomorphological mapping provides insights into the Quaternary landscape evolution of the Gulf of Corinth, Greece

Sofia Rossi, Konstantinos Tsanakas, Monica Giona Bucci, Dimitris Sakellariou, Mauro Soldati & Efthimios Karymbalis

To cite this article: Sofia Rossi, Konstantinos Tsanakas, Monica Giona Bucci, Dimitris Sakellariou, Mauro Soldati & Efthimios Karymbalis (2026) Integrated terrestrial and submarine geomorphological mapping provides insights into the Quaternary landscape evolution of the Gulf of Corinth, Greece, Journal of Maps, 22:1, 2621506, DOI: 10.1080/17445647.2026.2621506

To link to this article: https://doi.org/10.1080/17445647.2026.2621506

JOURNAL OF MAPS
2026, VOL. 22, NO. 1, 2621506
https://doi.org/10.1080/17445647.2026.2621506

SCIENCE

OPEN ACCESS Check for updates

Integrated terrestrial and submarine geomorphological mapping provides insights into the Quaternary landscape evolution of the Gulf of Corinth, Greece

Sofia Rossi [a,b], Konstantinos Tsanakas [c], Monica Giona Bucci [d,e], Dimitris Sakellariou [f], Mauro Soldati [a] and Efthimios Karymbalis [c]

[a]Department of Chemical and Geological Sciences, University of Modena and Reggio Emilia, Modena, Italy; [b]School of Advanced Studies (IUSS), Pavia, Italy; [c]Department of Geography, Harokopio University of Athens, Kallithea, Greece; [d]Marine Geology and Seafloor Surveying Group, University of Malta, Msida, Malta; [e]R3Vox, Mdina Road, Central Business District, Birkirkara, Malta; [f]Hellenic Centre for Marine Research, Anavyssos, Greece

ABSTRACT

This study presents a 1:150,000 scale geomorphological map of the Gulf of Corinth (central Greece), integrating terrestrial and submarine landforms. The Gulf, an asymmetric WNW-ESE half-graben, is one of the tectonically most active areas in the eastern Mediterranean, with an uplifting southern flank and a downward flexed northern one. A multidisciplinary approach, combining field surveys and high-resolution seafloor bathymetry, was used to map the emerged and submerged geological and geomorphological features. The southern terrestrial sector shows clear evidence of tectonic uplift, such as marine terraces, elevated Gilbert deltas, tidal notches at higher elevations, and reversed drainage features. In contrast, the northern part is notable for the absence of Quaternary marine or lacustrine sediments and displays a gently sloping shelf with submerged tidal notches, indicating ongoing tectonic subsidence. The map offers a comprehensive view of the complex geomorphology of the region, shaped by Quaternary tectonic activity.

ARTICLE HISTORY
Received 30 April 2025
Revised 6 January 2026
Accepted 15 January 2026

KEYWORDS
Integrated geomorphological map; emerged and submerged landforms; tectonic activity; Gulf of Corinth; Greece

1. Introduction

Integration of terrestrial and submarine geomorphological data is critical for understanding the connections between inland and seafloor landscapes (Prampolini et al., 2020). This approach enables the creation of detailed integrated geomorphological maps, which improve scientific understanding of the dominant coastal processes and the palaeogeographic evolution of coastal regions . In addition to their scientific values, integrated geomorphological maps have practical applications in fields such as environmental conservation, spatial planning and disaster risk management in tectonically active and climate-sensitive coastal regions.

Traditionally, terrestrial and marine landscapes have been studied independently, with research focusing either onshore, including coastal zones, or offshore (Goswami et al., 2017; Mayer et al., 2018; Prampolini et al., 2020; Sandwell et al., 2003; Wölfl et al., 2019 and references therein). Geomorphological mapping of terrestrial regions has long been a key method for studying onshore landforms, facilitated by Geographic Information Systems (GIS) and remote sensing technologies, which provide readily available datasets, including high-resolution Digital Elevation Models (DEMs) and Digital Terrain Models (DTMs). These advanced approaches, combined with field observations, have made possible the extensive production of geomorphological maps across various terrestrial regions globally, including diverse landscapes in Greece (Karymbalis et al., 2013; Karymbalis et al., 2016a; Tsanakas et al., 2019; Tsanakas et al., 2025). Conversely, mapping underwater landforms has lagged behind due to the technical challenges of seafloor research, which is why only a portion of the world's seabed has been thoroughly explored (Mayer et al., 2018 and references therein; Wölfl et al., 2019), despite breakthroughs in underwater exploration and mapping methods, such as submarine acoustic remote sensing and marine robotics (Sandwell et al., 2003). Traditionally, mapping underwater landforms has relied on acoustic methodologies such as single beams, side scan sonars, and multibeams. However, the high costs related to the mobilization of these devices have historically slowed progress in submarine geomorphic mapping. The emergence of high-resolution acoustic techniques including LiDAR (Foglini et al., 2016; Terefenko et al., 2018; Tiede et al., 2023), drone technology (Alevizos & Alexakis, 2022; Casella et al., 2016; Taddia et al., 2020), and satellite

CONTACT Sofia Rossi sofia.rossi@unimore.it Department of Chemical and Geological Sciences, University of Modena and Reggio Emilia, Modena, Italy

Supplemental data for this article can be accessed online at https://doi.org/10.1080/17445647.2026.2621506.

derived bathymetry (Darmanin et al., 2023; Sagawa et al., 2019; Susa, 2022; Tang & Mahmud, 2021), has significantly advanced the mapping of coastal regions and submarine geomorphic features in depths of up to -30 m. This is demonstrated by recent integrated coastal and marine geohazard mapping efforts (e.g. Gamberi et al., 2024; Orrù et al., 2024). These new technologies have encouraged scientists to work toward obtaining more comprehensive high-resolution datasets in a wide range of research areas. These include geoarchaeology (Harff et al., 2016; Sakellariou & Galanidou, 2016; Mattei et al., 2018; Tsakanikou et al., 2021), Quaternary geology and reconstruction of the palaeogeographic evolution of coastal regions (Deiana et al., 2021; Guida & Valente, 2019; Miccadei et al., 2012; Prampolini et al., 2017, 2018; Savini et al., 2021; Soldati et al., 2021), geoheritage (Coratza et al., 2019), and coastal risk mitigation (Gianardi et al., 2024; Parrott et al., 2008; Vandelli et al., 2023). Nevertheless, in deeper marine settings, high-resolution multibeam bathymetry remains the most reliable tool for detailed seafloor characterization. In this study, we build upon existing and newly acquired multibeam datasets to provide an integrated geomorphic analysis of the Gulf of Corinth, taking advantage of recent improvements in multibeam technology and data resolution.

The Gulf of Corinth is located in central Greece, in the western part of the Aegean microplate, above the Hellenic subduction zone and between the opposite tips of two major dextral strike-slip, the Kephallinia and the North Anatolian fault zones (Papanikolaou & Royden, 2007; Sakellariou & Tsampouraki-Kraounaki, 2019) (Figures 1a and b). It is a globally significant site for studying intracontinental rifting and normal fault mechanics due to its rapid extension and high seismic activity (Armijo et al., 1996; Avallone et al., 2004; Nixon et al., 2024; Reilinger et al., 2009) (Figure 1b). The main objective of this study is to present the first integrated geomorphological map of the terrestrial and submarine landscapes of the Corinth Rift at a scale of 1:150,000 (Main Map). The integration of submarine dataset together with onshore information is the first step towards an improved understanding of its tectonic activity. Although de Gelder et al. (2019) combined onshore high-resolution topography with offshore seismic data to constrain the mechanics of the Corinth Rift across various timescales, no previous attempts are available, to present a comprehensive geomorphological overview of the Rift's land-sea continuum.

2. Regional and geotectonic setting of the study area

The Corinth Rift, an amagmatic rift stretching 150 km in a WNW-ESE direction across central Greece (Figure 1b), separates mainland Greece to the north from the Peloponnese to the south (Armijo et al., 1996; Fernández-Blanco et al., 2019). This graben shapes the Gulf of Corinth, a narrow marine basin that is approximately 30 km wide and descends to a maximum depth of 870 m. The southern coast of the Gulf is sharp and linear, contrasting with the more irregular northern one, characterized by bays and peninsulas. To the west, it connects to the Gulf of Patras through the Rio – Antirio Strait (2 km wide, 65 m deep), while to the east it links to the Saronikos Gulf via the artificially dredged Corinth Canal (6 km long, 21 m wide, 8 m deep) (Figure 1a). At its eastern extremity, the Gulf divides into two sub-basins, the Alkyonides Gulf and the Lechaion Gulf, separated by the Perachora Peninsula (Figure 1a).

In this structural context, the geomorphological map covers both the Gulf's seafloor and the surrounding catchments areas of the drainage networks that discharge sediment into it (Figure 1a), directly linked to the basin evolution. The study area consists of the pre-rift 'Alpine' basement (Hellenides) and syn-rift 'post-Alpine' formations. Pre-rift rocks, mainly Mesozoic carbonate, siliceous rocks and flysch, belong to the geotectonic units of Gavrovo-Tripolis, Olonos-Pindos, Parnassos-Ghiona, Sub-Pelagonic, and Boetian Series. In the North Peloponnese, syn-rift Pliocene-Pleistocene deposits (interbedded conglomerates, marls, sandstones, and clays) overlie the pre-rift basement, while syn-rift formations are absent north of the Gulf.

3. Materials and methods

The geomorphological mapping conducted for this study was performed based on a multidisciplinary approach as shown in Figure 2, combining the analysis and interpretation of high-resolution bathymetry datasets and remote-sensed images with field surveys in selected areas. The interpretation of aerial photos taken in 1996, along with freely available satellite data web services such as Google Earth Pro and ESRI World Imagery, was helpful in identifying terrestrial landforms. Moreover, for mapping the terrestrial landforms and extracting the drainage network, a 25 m resolution DEM of the terrestrial area was produced, resampled from a 5 m DEM from the Hellenic Cadastre and aligned with the 25 m resolution of the Gulf's seafloor DEM used for mapping the submerged landforms (Figure 3a). The bathymetric surveys of the Gulf of Corinth were conducted during multiple campaigns of the HCMR's vessel R/V 'AEGAEO' between March 2001 and November 2004, using the 20 kHz SEABEAM 2120 system (Nomikou et al., 2011; Sakellariou et al., 2011). Additionally, we compiled the submarine mapping with a new 10 m resolution bathymetric layer, collected during the M196 expedition in December 2023. This layer was

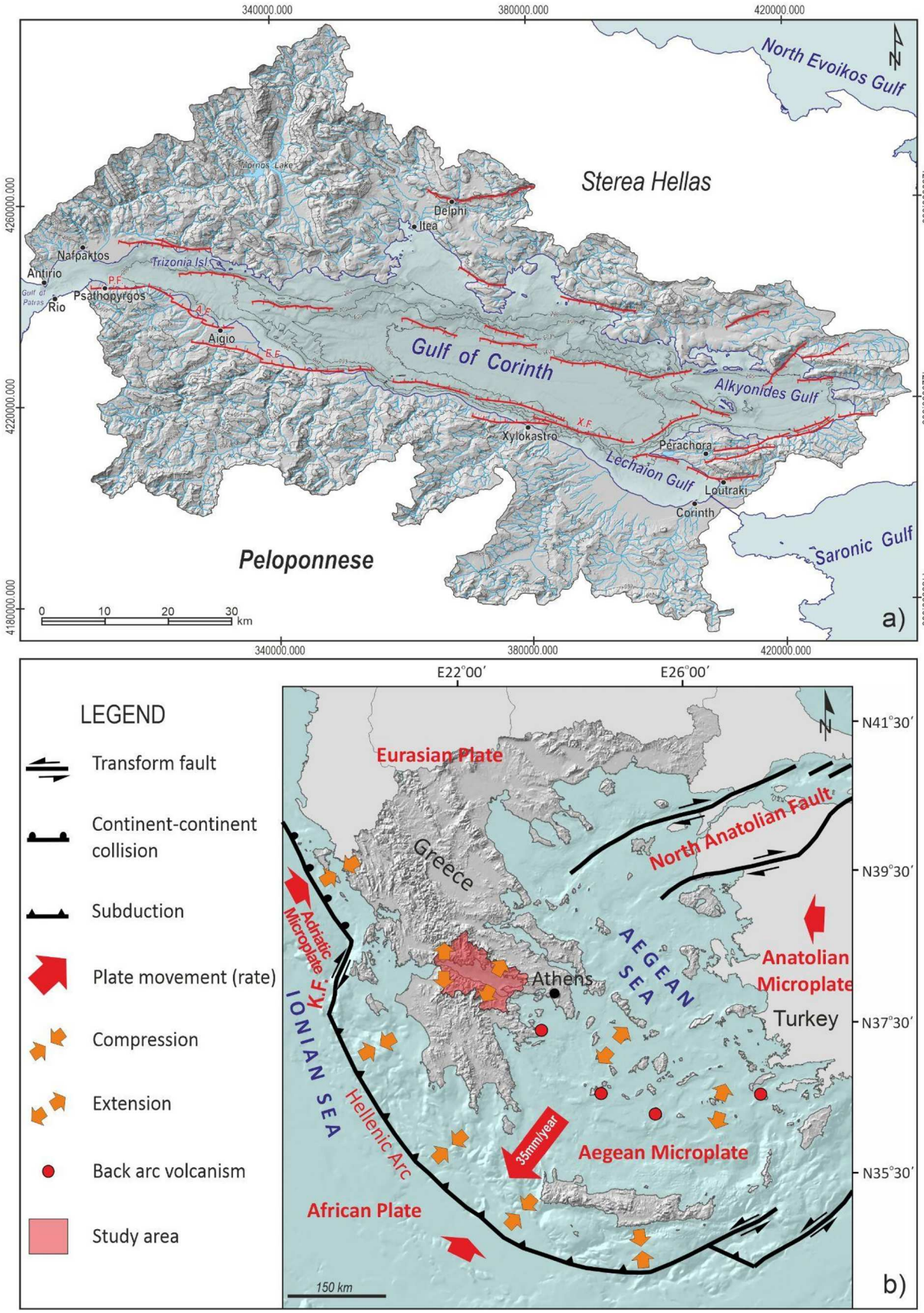

Figure 1. (a) Map of the study area; red lines correspond to the major faults of the Corinth Rift; P.F.: Psathopyrgos fault; A.F.: Aigion fault, E.F.: Eliki fault, and X.F.: Xylokastro fault. (b) Geotectonic setting of the study area; K.F.: Kephallinia fault.

produced through integrated multibeam surveys conducted using the EM710 and EM122 systems (Jegen et al., 2024).

Various elevation derivatives such as hillshade map, slope map and red relief image map (RRIM), and hydrological attributes such as flow direction were

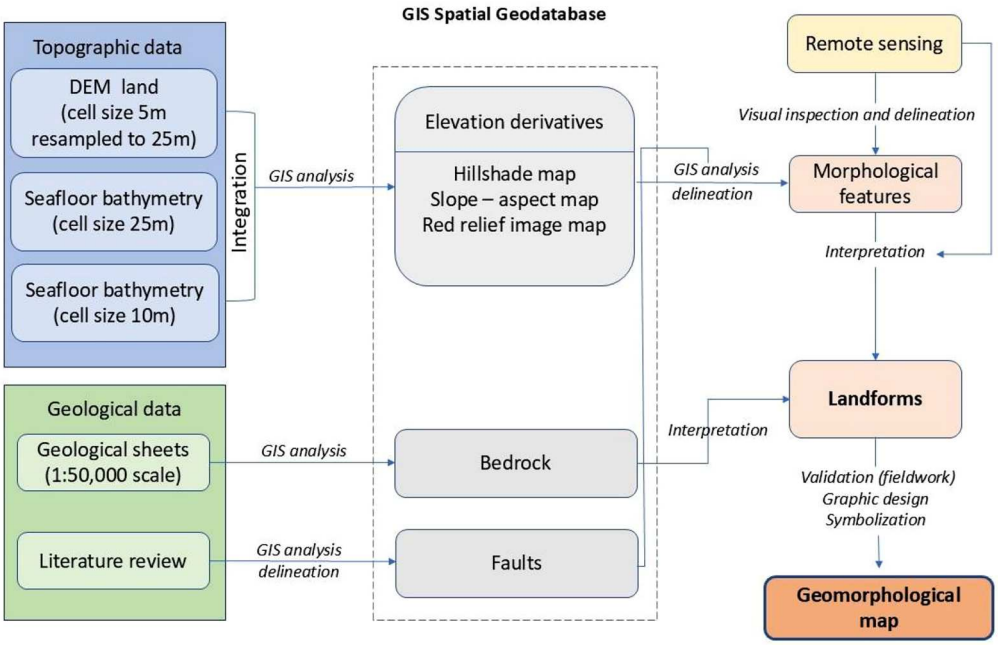

Figure 2. The flowchart illustrates the methodological approach adopted to produce the integrated geomorphological map of the Gulf of Corinth.

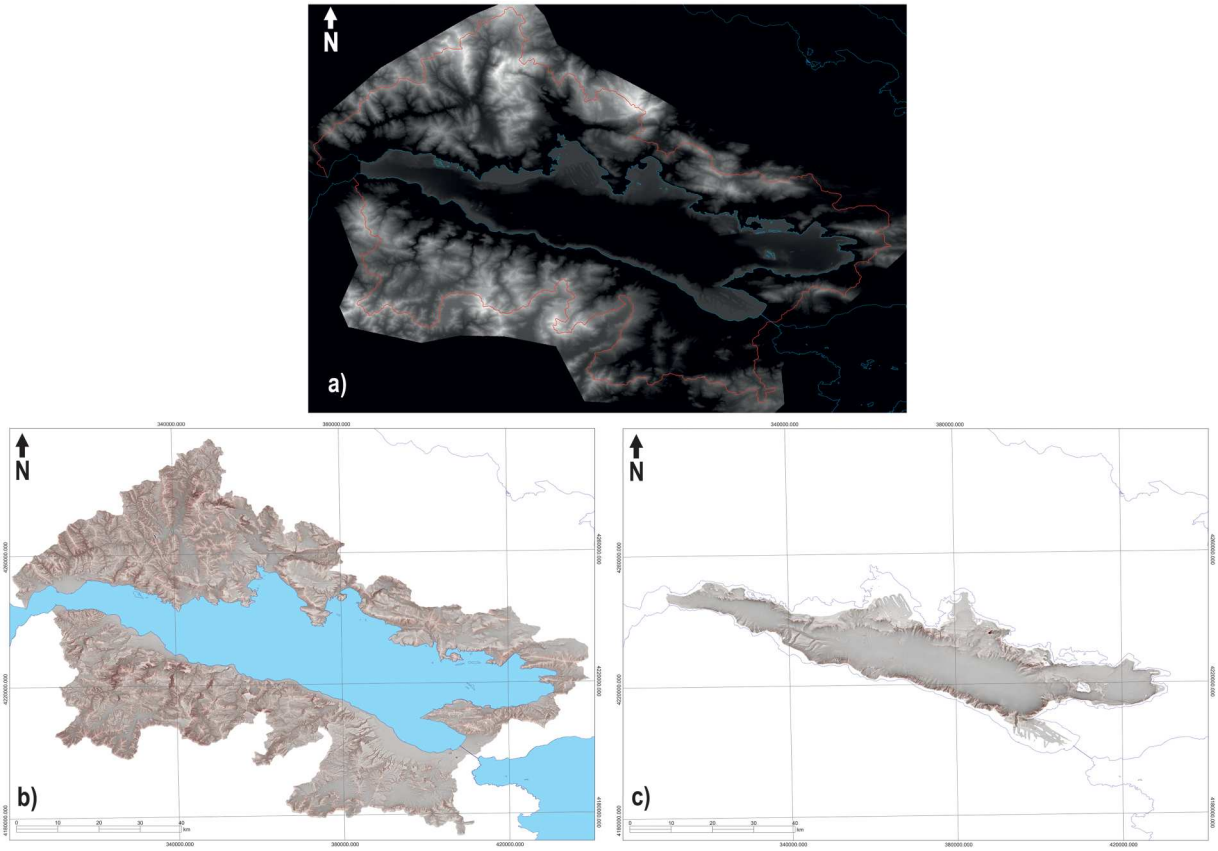

Figure 3. (a) The 25 m resolution land DEM aligned with the 25 m resolution bathymetry; the red line marks the study area and the blue line shows the coastline. (b-c) The subaerial (b) and submarine (c) red relief image map (RRIM) of the study area.

exploited to identify and map terrestrial and submarine landforms. Among these, the RRIM (Figures 3b and c) was especially effective in visualizing the surface morphology of the area by creating a 3D visualization that distinctly differentiates land surface and seafloor features (Daxer, 2020; Tzvetkov, 2018) without directional bias. The RRIM combines the topographic slope with the Ridge and Valley index (RV_i) (Chiba et al., 2008), an index calculated considering the positive and negative openness as defined by Yokoyama et al.

(2002). The RRIM uses red for steep slopes and grey for flat surfaces, facilitating the identification of features such as crests, structural and erosional scarps, valleys, gorges and gullies, and gently sloping landforms like marine and fluvial terraces, alluvial fans, fan deltas, dolines and poljes.

The landforms are categorized by their genetic processes into structural, coastal, marine, gravity-induced, karst, fluvial and glacial groups. Symbols and colors follow the Geological Survey of Italy standards (cf. Campobasso et al., 2021), with minor modifications for sake of clarity. The geological formations are delineated using 24 geological maps at a 1:50,000 scale provided by the Greek Institute of Geology and Mineral Exploration. The bedrock, regardless of age, is classified into eight lithological groups: bauxite, metamorphic rocks, igneous rocks, carbonate sedimentary rocks, siliceous sedimentary rocks, flysch, marls-sandstones-clays, and conglomerates. Fault mapping, which focused on both onshore and offshore tectonic structures of the Rift, is derived from a range of previous studies (Bussolotto et al., 2015; Dart et al., 1994; Fernández-Blanco et al., 2019; Karymbalis et al., 2018; Maroukian et al., 2008; Roberts et al., 2009; Sakellariou et al., 2007 and references therein).

4. Results

The integrated geomorphological map of the Gulf of Corinth was compiled at the scale of 1:150,000 (Main Map). The selected scale allows the full extent of the drainage basins discharging into the Gulf to be considered, offering a comprehensive view of the region. Although minor landforms cannot be mapped in detail, this scale ensures sufficient regional coverage and readability of the major features. Below, geomorphological features are described according to their genesis.

4.1. Structural elements and landforms

The most pronounced structural elements and landforms in the study area are the active normal faults, and the cliffs and scarps they have created. Currently, fault activity is concentrated in the submarine rift and along the southern Gulf coast (Stefatos et al., 2002) (Figure 4a). Rift border faults, arranged in enéchelon segments approximately 10–25 km in length, have a cumulative length of ~130 km. Their along-rift strikes vary from NE-SW to ENE-WSW in the easternmost Rift, shifting to WNW-ESE to E-W in the central and west Rift. Farther to the south, older Quaternary normal faults exhibit orientation similar to those at the current Rift edge but show little evidence of recent activity. Seismic and morphological data suggest that these faults are less active, indicating a northward migration of both fault activity and the Rift southern boundary. In addition, active normal faults and associated cliffs and scarps are present on the northern side of the Gulf with the most important being the Marathias, Delphi (Figure 4b), and Kaparelli faults.

The most pronounced tectonic knickpoints were identified along the rivers of the North Peloponnese, south of the Gulf (Figure 4c). Their spatial distribution is controlled by variation in tectonic uplift rates. In the eastern Rift, knickpoints were mapped at low elevations (100–200 m a.s.l.), with additional ones identified at higher elevations (~275 m, ~450 m, and ~700 m a.s.l.). The central Rift features the steepest and shortest river profiles, with multiple knickpoints at ~100–200 m, ~1,100–1,200 m, and ~1,500–1,700m a.s.l.. In the western Rift long and short stream profiles alternate, with knickpoints at varying elevations. Rivers draining the footwall of the Eliki fault have four knickpoints, mostly at ~100–200 m a.s.l., while those draining the uplifting block of the Aigio fault lack low-elevation knickpoints but exhibit tectonic knickpoints aligned with those at the highest elevations to the east (Fernández-Blanco et al., 2019; Karymbalis et al., 2016b).

4.2. Coastal elements and landforms

Marine terraces serve as key indicators of tectonic uplift in the study area (Armijo et al., 1996; de Gelder et al., 2019). Uplifted terrace sequences have formed along the southern margin of the Rift, from Alepochori to Psathopyrgos, with the best-preserved examples west of Corinth, extending 40 km along the Gulf (Figure 4d). These terraces, carved into Plio-Pleistocene marls, have been dated to late Pleistocene sea-level high stands (Armijo et al., 1996; de Gelder et al., 2019; Maroukian et al., 2008), some reaching 400 ka. This age reference is based on sea-level correlations and previously published geomorphological interpretations, and therefore involves inherent uncertainties that may be refined as new geochronological data become available. The elevation of the marine terraces increases toward the north-west, with up to 14 terraces along the Xylokastro fault, the highest at ~400 m a.s.l. (Armijo et al., 1996; de Gelder et al., 2019). Similar sequences occur along the Eliki, Aigio, and Psathopyrgos faults, with inner edges of MIS 5e terraces ranging from 90 to 177 m a.s.l.. On the Perachora peninsula and in Alepochori, terraces at ~30 m a.s.l. suggest uplift rates of approximately 0.18 and 0.3 mm/yr, respectively (Leeder et al., 2003; Maroukian et al., 2008).

Uplifted syn-rift Plio-Pleistocene Gilbert-type fan deltas stretch along the southern edge of the Rift (Seger & Alexander, 2009). These fan deltas rest unconformably atop Pliocene-Pleistocene formations, and in some cases even older Mesozoic rocks

Figure 4. (a) Xylokastro fault plane in its onshore segment. The fault cuts Mesozoic limestones. View from east (left) to west (right); (b) Delphi fault scarp. The fault cuts Mesozoic limestones. View from west (left) to east (right); (c) Knickpoint at the upper reaches of the Dervenios River; (d) Sequence of uplifted marine terraces, northern Peloponnese. View from east (left) to west (right); (e) Uplifted Gilbert fan delta foreset deposits, Evrostini. View from south (left) to north (right); (f) Uplifted tidal notches, Cape Heraion, Perachora Peninsula. View from SE (left) to NW (right); (g) Series of 4 uplifted tidal notches, Mylokopi, Perachora Peninsula. View from SW (left) to NE (right).

(Gawthorpe et al., 2017; Ori, 1989). Six Pleistocene fan deltas are identified from east to west: Klimenti, Evrostini, Platanos, Vouraikos, Kolokotronis, and Meganitis. The fan deltas of Evrostini (Figure 4e) and Klimenti, are uplifted by fault activity, reaching elevations of up to 1,200 m a.s.l., while the topset deposits of the Late Pliocene Mavro Oros fan delta in north-central Peloponnese reach a thickness of over 700 m and are elevated up to 1,756 m a.s.l. (Fernández-Blanco et al., 2019). Both the thickness and elevation of these deposits highlight significant tectonic uplift in the region.

Elevated tidal notches in Mesozoic limestone cliffs at Cape Heraion on the Perachora Peninsula (Figure 4f) provide evidence of Late Holocene coseismic uplift (Kershaw & Guo, 2001; Pirazzoli et al., 1994). Four well-preserved notches, ranging from +1.1 to +3.2 m a.s.l., indicate seismic events, with the oldest dated to 4,440–4,320 BC and the most recent to 190–440 AD (Pirazzoli et al., 1994). Similar uplifted notches appear in Mylokopi (Figure 4 g), while Psatha Bay hosts three bioerosional notches, the highest at ~2 m a.s.l., suggesting a tectonic uplift rate of ~0.3 mm/yr over 7,000 years (Leeder et al., 1991). In contrast, submerged tidal notches in Itea and Antikyra, at depths of −50 to −20 cm b.s.l., are indicative of recent coseismic subsidence (Evelpidou et al., 2011).

4.3. Marine elements and landforms

The Gulf of Corinth's main basin reaches depths of 800–900 m b.s.l., and shows a flat, ellipsoidal shape covering 637 km². The basin is defined by major east–west faults and erosional scarps, prominent along its western side (Figure 1a). This submarine landscape is dominated by mass transport deposits and gullies, with many of them along the Gulf's margins. Gullies are densely concentrated in the southwest, where steeper slopes create a complex network of canyons, channels, and terraces across the Gulf floor (Figures 5a and b). Single-channel canyons of varying lengths outline the Gulf, with several extending from the southern margin toward the basin center, especially in the west (Figure 5b). Sediment waves appear on the western and eastern sides at depths of 230–240 m b.s.l., while numerous cyclic steps are scattered along the southern and western margins. A pockmark field is present in the south-western area of the Gulf, while contourite-related depressions are observed in the north-central basin.

4.4. Gravity-induced landforms

Gravity-induced landforms are widespread throughout the Gulf of Corinth and its surroundings, representing one of the clearest expressions of the geomorphological continuity between terrestrial and submarine landscapes. Onshore, landslides are particularly frequent along the western part of the study area, affecting both the northern and southern margins of the Gulf. Their occurrence is driven by frequent seismic activity and heavy rainfall (Koukis et al., 2009). In addition, the presence of alternating soft and hard rock layers with varying permeability and geotechnical properties favors such events, especially where strata orientation aligns with steep slopes (Chalkias et al., 2016). Major landslides are those of Marathias (Figure 6a) and Sergoula (Figure 6b) on the north-west coast, and Panagopoula on the south-west coast of the northern Peloponnese. These deep-seated rotational rock slides are linked to active faults, were triggered by earthquakes and often reactivated during periods of intense rainfall (Gallousi & Koukouvelas, 2007). It is interpreted that their landslide deposits were reworked by torrent producing large debris- flow dominated fans (Figure 6b). Gravity-driven processes continue offshore through the development of submarine landslide scarps, mass transport deposits and debris flows. These features are particularly common in the central-western part of the Gulf, where landslide scarps are observed at depths ranging from approximately 170–620 m b.l.s, often aligned with major tectonic structures. In several areas, submarine landslide deposits merge into isolated bathymetric highs and transition downslope into debris-flow systems, especially in the south-west sector.

4.5. Karst landforms

The central and eastern parts of the northern section of the study area host diverse karst landforms developed on Mesozoic carbonate rocks of the Parnassos-Giona unit (Papadopoulou-Vrynioti & Bellos, 2001). Poljes, with E-W and NW-SE axes, are found on Mounts Parnassos and Elikonas, and at the western slopes of Mount Giona, at elevations ranging between 96 and 1493 m a.s.l. (Figure 6c). These poljes are polygenetic features, formed by chemical erosion during the Miocene-Pliocene and influenced by NW-SE trending faults (Papadopoulou-Vrynioti & Bellos, 2001). An exceptional karst landform, the Corycian Cave (Figure 6d) on Mount Parnassos at 1,360 m a.s.l., features two large caverns adorned with stalactites and stalagmites, along with evidence of Neolithic human habitation. At elevations above 1,000 m a.s.l., particularly on Mount Elikonas and Mount Parnassos, doline fields form high karst cockpit-doline landscapes. These dolines are recent and represent an early stage of karst evolution while their characteristics are controlled by tectonics. Beyond these fields, multiple solutional and collapse dolines are scattered across exposed limestone areas (Figures 6e and f). Bauxite outcrops in the study area are linked to

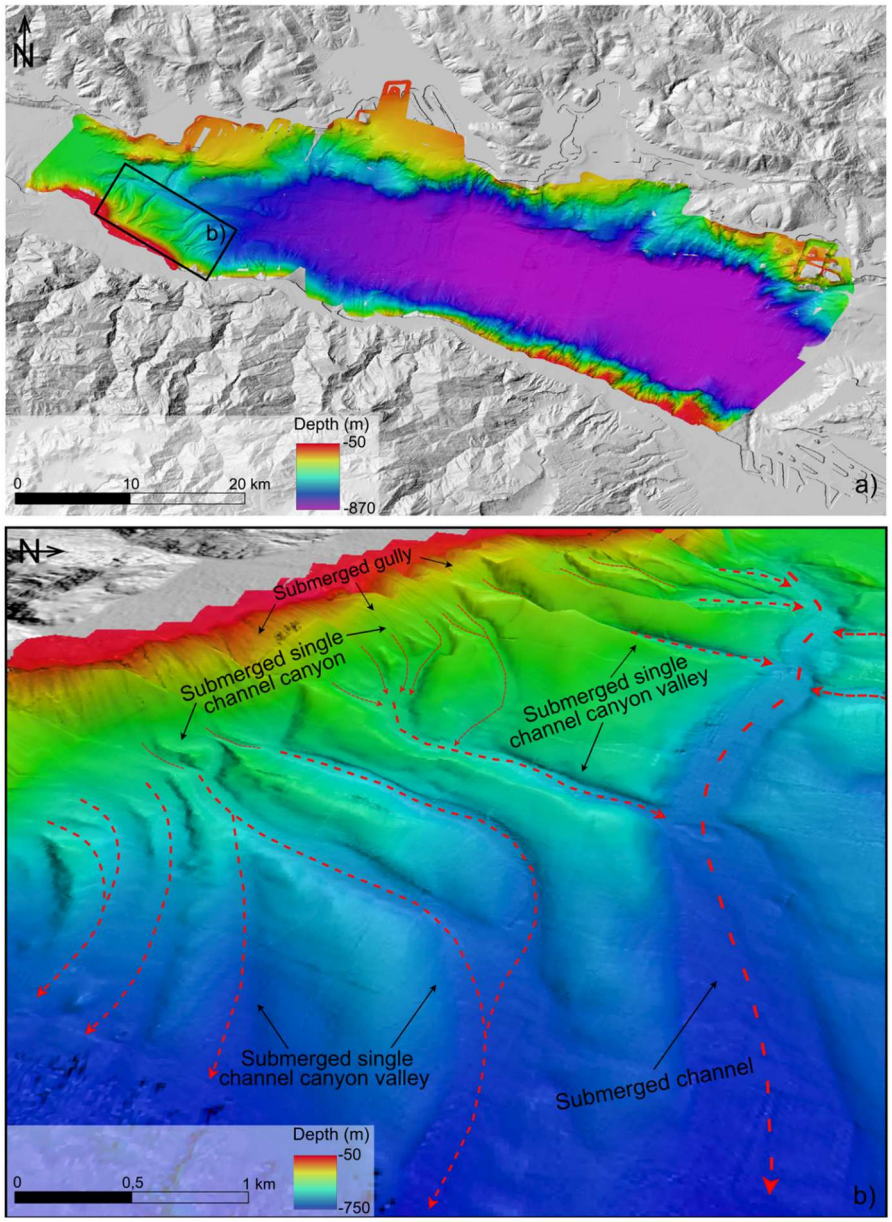

Figure 5. (a) The 10 m resolution bathymetry used for mapping marine elements and features; the black box indicates the location of the area shown in (b). (b) High-resolution bathymetric detail of the south-western sector of the Gulf highlighting submarine erosional landforms, including submerged gullies, single-channel canyons, and canyon valleys.

paleokarst, as they were deposited in cockpit-doline depressions from the Middle Jurassic to the Late Cretaceous (Mondillo et al., 2022). These karst depressions were formed during brief emersion periods when carbonate rocks were exposed to freshwater, leading to dissolution and karstification.

4.6. Fluvial landforms

In the study area, intense fluvial incision driven by tectonic uplift has shaped steep-sloped valleys and impressive gorges. In northern Peloponnese, the largest gorges have been carved by the Vouraikos (Figure 7a), Selinountas, and Krathis rivers, cutting deep into Mesozoic limestone. In the northern part of the study area, channel downcutting by the Rekkas stream has formed a deep gorge stretching approximately 10 km (Figure 7b).

The presence of easily erodible poorly cemented marls, combined with tectonic uplift and high rainfall, led to the development of a badland landscape in the central region, around Lykoporia and south to south-west of Xylokastro (Figures 7c and d), as well as in the western part of northern Peloponnese (along the north-western foothills of Mount Panachaiko).

Wind gaps were also recognized in the study area, resulting from the inversion of the drainage network induced by the intense tectonic uplift (Figure 7e). These are particularly evident in the central sector of the southern margin of the Gulf, which is characterised by evident palaeo-flow directions.

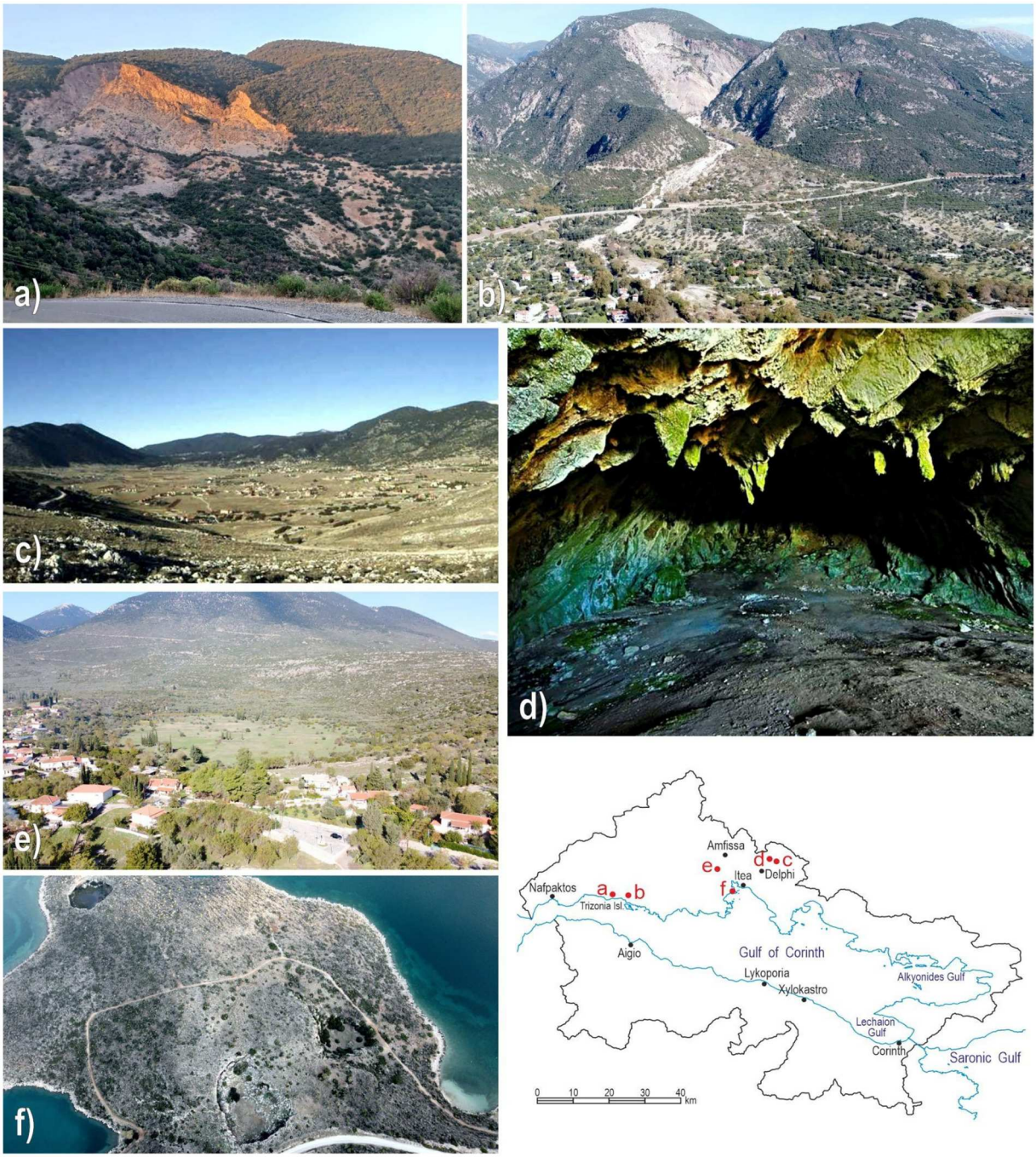

Figure 6. (a) Marathias landslide. View from north (left) to south (right); (b) Sergoula landslide and debris-flow dominated fan. View from NW (left) to SE (right); (c) Livadi polje. View from SW (left) to NE (right); (d) Corycian cave; (e) Solution sinkhole at Aghia Efthimia. View from NW (left) to SE (right); (f) Collapse sinkholes between Galaxidi and Itea. View from ENE (left) to WSW (right).

5. Discussion and conclusions

This study represents the first attempt to create a unified geomorphological map of the Corinth Rift and its surrounding regions, incorporating both the terrestrial and submarine landforms. The integration of land and marine investigations was essential for advancing our understanding of the geomorphic evolution of the study area. Combined mapping in the Gulf of Corinth highlights how fluvial and neotectonic processes shape the modern coastline. The same tectonic structures that control the coastline continue on the seabed. Ongoing Rift activity is evidenced by the presence of E-W and ESE-WNW striking active normal faults, both onland and offshore. Moreover, the occurrence of both terrestrial and submarine terraces illustrate the continuity of geomorphic processes across onshore and offshore environments (see geomorphological cross-section ABC on the Main Map). Indicators of mass transport are observed on land through numerous landslide scarps, alluvial fans, and debris flows. In the submarine domain, similar processes are reflected in submerged landslide-deposit sediment waves, and

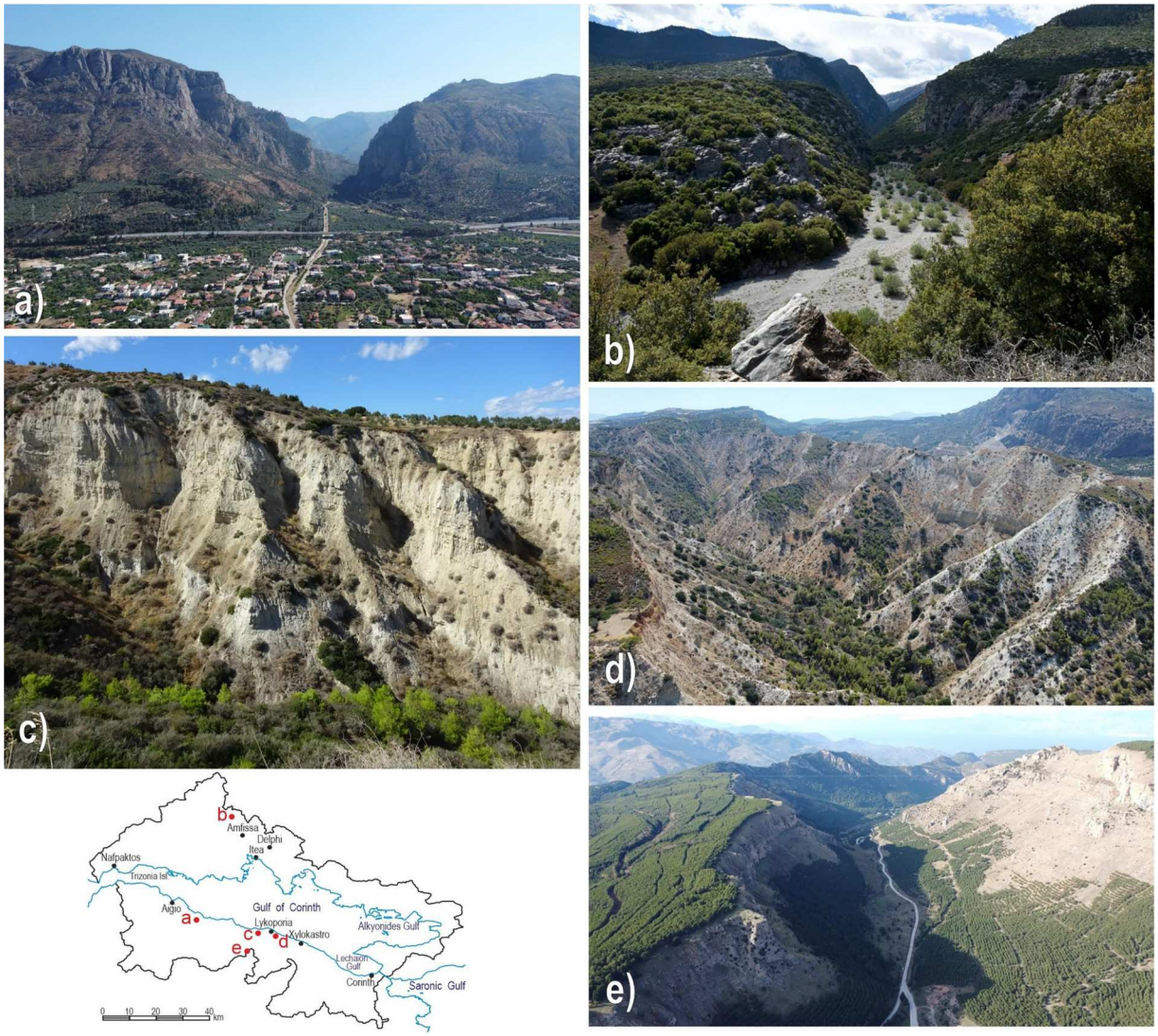

Figure 7. (a) Vouraikos River gorge, north Peloponnese. View from east (left) to west (right); (b) Rekkas Stream gorge. View from south (left) to north (right); (c) Badland landscape, south of Lykoporia. View from south (left) to north (right); (d) Badland landscape, south-west of Xylokastro. View from SW (left) to NE (right); (e) Wind gap in northern Peloponnese associated with the Dervenios and Olvios drainage reversal. View from west (left) to east (right).

gullies, all pointing to the active role of gravity driven flows. The submerged canyons and fans display the same morphostructural trends as the emerged fluvial features. South of the Gulf, the presence of marine terraces up to approximately 400 m a.s.l., Gilbert-type fan delta deposits at high elevations (reaching 1,756m a.s.l.), uplifted tidal notches, and the narrow and steep continental slope are indicative of high rates of continuous tectonic uplift during the Quaternary. Conversely, the absence of Quaternary marine or lacustrine sediments, the wider and gently dipping continental shelf with a less steep continental slope, and the presence of submerged tidal notches in the northern part of the study area are the result of tectonic subsidence. The type of recognized deposits represented in the geomorphological map indicates that the majority of the seafloor landforms formed in an underwater environment. The Main Map depicts the spatial distribution of submarine elements and landforms comprehensively, and can contribute to more in-depth studies on the paleoenvironmental conditions that led to their formation. This study provides a foundation for hazard assessment, especially in Mediterranean coastal areas affected by sea-level rise, and in submarine regions undergoing coastal erosion and mass movements. Although coastal risk modeling is beyond the scope of this work, we provide a spatial identification of active faults, active landslides, uplifted sectors, subsiding coasts, and erosion-prone slopes. This information can represent a fundamental cartographic and interpretative basis for local authorities responsible for risk mitigation and coastal zone planning in tectonically active regions.

Software

The Main Map and its final layout were produced using ESRI ArcGIS Pro 3.4 and CorelDRAW Graphic Suite 2023. ArcGIS Pro was employed for the spatial analysis and cartographic rendering of geomorphological features, while CorelDRAW was used to refine

the visual layout and incorporate graphical elements. Within the map, the legend of geomorphological features and a geodynamic framework were added, alongside the map title and author details. The symbology applied follows the guidelines proposed by the Geological Survey of Italy (cf. Campobasso et al., 2021), which recommend the representation of landforms and associated deposits using symbols of different colors according to geomorphological processes that led to their genesis.

Acknowledgements

We extend our sincere appreciation to the entire scientific team of the M196 Cruise, conducted aboard the RV Meteor, in December 2023.

This paper and related research have been conducted during and with the support of the Italian inter-university PhD course in Sustainable development and climate change (www.phd-sdc.it).

Disclosure statement

No potential conflict of interest was reported by the author(s).

Data availability statement

The base map of the land area is a 25-m resolution Digital Elevation Model (DEM) obtained by resampling a 5-m DEM from the Hellenic Cadastre and aligned with a 25-m DEM of the seafloor. The bathymetric data were collected during oceanographic surveys conducted by HCMR's R/V AEGAEO between March 2001 and November 2004, using the SEABEAM 2120 system (20 kHz).

Terrestrial landform mapping was supported by remotely sensed images dated 1996, available for public consultation and download via Google Earth Pro (https://www.google.com/earth/versions/#earth-pro) and ESRI World Imagery (https://www.arcgis.com/home/item.html?id=10df2279f9684e4a9f6a7f08febac2a9) platforms.

Submerged landform mapping was refined using a 10-m resolution DEM derived from multibeam echosounder surveys (EM710 and EM122 systems) conducted during the M196 expedition in December 2023.

The data obtained in this study are available from the corresponding author [SR], upon reasonable request. Requests for data will be assessed on a case-by-case basis to ensure compliance with ethical, privacy, and security considerations.

ORCID

Sofia Rossi https://orcid.org/0009-0009-6140-1610
Konstantinos Tsanakas https://orcid.org/0000-0002-6516-9929
Monica Giona Bucci https://orcid.org/0000-0002-4924-6488
Dimitris Sakellariou https://orcid.org/0000-0002-2982-4375
Mauro Soldati http://orcid.org/0000-0002-1600-4255
Efthimios Karymbalis https://orcid.org/0000-0003-3355-6657

References

Alevizos, E., & Alexakis, D. D. (2022). Monitoring short-term morphobathymetric change of nearshore seafloor using drone-based multispectral imagery. *Remote Sensing*, *14*(23), 6035. https://doi.org/10.3390/rs14236035

Armijo, R., Meyer, B. G. C. P., King, G. C. P., Rigo, A., & Papanastassiou, D. (1996). Quaternary evolution of the Corinth Rift and its implications for the Late Cenozoic evolution of the Aegean. *Geophysical Journal International*, *126*(1), 11–53. https://doi.org/10.1111/j.1365-246X.1996.tb05264.x

Avallone, A., Briole, P., Agatza-Balodimou, A. M., Billiris, H., Charade, O., Mitsakaki, C., Nercessian, A., Papazissi, K., Paradissis, D., & Veis, G. (2004). Analysis of eleven years of deformation measured by GPS in the Corinth Rift laboratory area. *Comptes Rendus, Geoscience*, *336*(4-5), 301–311. https://doi.org/10.1016/j.crte.2003.12.007

Bussolotto, M., Benedicto, A., Moen-Maurel, L., & Invernizzi, C. (2015). Fault deformation mechanisms and fault rocks in micritic limestones: Examples from Corinth rift normal faults. *Journal of Structural Geology*, *77*, 191–212. https://doi.org/10.1016/j.jsg.2015.05.004

Campobasso, C., Carton, A., Chelli, A., D'Orefice, M., Dramis, F., Graciotti, R., Guida, D., Pambianchi, G., Peduto, F., & Pellegrini, L. (2021). Aggiornamento ed Integrazioni delle Linee Guida della Carta Geomorfologica d'Italia alla scala 1:50.000 e Banca Dati Geomorfologica – Progetto CARG: modifiche ed integrazioni al Quaderno n. 4/1994. *I Quaderni, serie III del Servizio Geologico d'Italia (SGI)*, *13*, 153.

Casella, E., Rovere, A., Pedroncini, A., Stark, C. P., Casella, M., Ferrari, M., & Firpo, M. (2016). Drones as tools for monitoring beach topography changes in the Ligurian Sea (NW Mediterranean). *Geo-Marine Letters*, *36*, 151–163. https://doi.org/10.1007/s00367-016-0435-9

Chalkias, C., Polykretis, C., Ferentinou, M., & Karymbalis, E. (2016). Integrating expert knowledge with statistical analysis for landslide susceptibility assessment at regional scale. *Geosciences*, *6*(1), 14. https://doi.org/10.3390/geosciences6010014

Chiba, T., Kaneta, S. I., & Suzuki, Y. (2008). Red relief image map: new visualization method for three dimensional data. The international Archives of the Photogrammetry. *Remote Sensing and Spatial Information Sciences*, *37*(B2), 1071–1076.

Coratza, P., Vandelli, V., Fiorentini, L., Paliaga, G., & Faccini, F. (2019). Bridging terrestrial and marine geoheritage: Assessing geosites in Portofino Natural Park (Italy). *Water*, *11*(10), 2112. https://doi.org/10.3390/w11102112

Darmanin, G., Gauci, A., Deidun, A., Galone, L., & D'Amico, S. (2023). Satellite-derived bathymetry for selected shallow Maltese coastal zones. *Applied Sciences*, *13*(9), 5238. https://doi.org/10.3390/app13095238

Dart, C. J., Collier, R. E. L., Gawthorpe, R. L., Keller, J. V. A., & Nichols, G. (1994). Sequence stratigraphy of Pliocene-Quaternary synrift, Gilbert-type fan deltas, northern Peloponnesos, Greece. *Marine and Petroleum Geology*, *11*, 545–560. https://doi.org/10.1016/0264-8172(94)90067-1

Daxer, C. (2020). Topographic openness maps and red relief image maps in QGIS. *Technol. Rep. Inst. Geol.*, *17*, 1–15. https://doi.org/10.13140/RG.2.2.18958.31047

de Gelder, G., Fernández-Blanco, D., Melnick, D., Duclaux, G., Bell, R., Jara-Muñoz, J., Armijo, R., & Lacassin, R. (2019). Lithospheric flexure and rheology determined

by climate cycle markers in the Corinth Rift. *Scientific Reports*, *9*, 4260. https://doi.org/10.1038/s41598-018-36377-1

Deiana, G., Lecca, L., Melis, R. T., Soldati, M., Demurtas, V., & Orrù, P. E. (2021). Submarine geomorphology of the Southwestern Sardinian Continental Shelf (Mediterranean Sea): Insights into the last glacial maximum sea-level changes and related environments. *Water*, *13*(2), 155. https://doi.org/10.3390/w13020155

Evelpidou, N., Pirazzoli, P. A., Saliege, J. F., & Vassilopoulos, A. (2011). Submerged notches and doline sediments as evidence for Holocene subsidence. *Continental Shelf Research*, *31*(12), 1273–1281. https://doi.org/10.1016/j.csr.2011.05.002

Fernández-Blanco, D., de Gelder, G., Lacassin, R., & Armijo, R. (2019). A new crustal fault formed the modern Corinth Rift. *Earth-Science Reviews*, *199*, 102919. https://doi.org/10.1016/j.earscirev.2019.102919

Foglini, F., Prampolini, M., Micallef, A., Angeletti, L., Vandelli, V., Deidun, A., Soldati, M., & Taviani, M. (2016). Late Quaternary coastal landscape morphology and evolution of the Maltese Islands (Mediterranean Sea) reconstructed from high-resolution seafloor data. *Geol. Soc. London*, 77–95. https://doi.org/10.1144/SP411.12

Gallousi, C., & Koukouvelas, I. K. (2007). Quantifying geomorphic evolution of earthquake-triggered landslides and their relation to active normal faults. An example from the Gulf of Corinth, Greece. *Tectonophysics*, *440*(1-4), 85–104. https://doi.org/10.1016/j.tecto.2007.02.009.

Gamberi, F., Casalbore, D., Marani, M., Rovere, M., Bosman, A., Calarco, M., Dalla Valle, G., Leidi, E., Martorelli, E., Mercorella, A., Pierdomenic, M., Romagnoli, C., Adami, C., Falese, F. G., Fascetti, A., Ferrante, V., Ingrassia, M., Lai, E., Montanaro, C., … Chiocci, F. L. (2024). Geohazard features of the Aeolian Island slopes and the North-Eastern Sicily offshore. *Journal of Maps*, *20*(1), 2343314. https://doi.org/10.80/17445647.2024.2343314

Gawthorpe, R. L., Andrews, J. E., Collier, R. E. L., Ford, M., Henstra, G. A., Kranis, H., Leeder, M. R., Muravchik, M., & Skourtsos, E. (2017). Building up or out? Disparate sequence architectures along an active rift margin – Corinth rift, Greece. *Geology*, *45*(12), 1111–1114. https://doi.org/10.1130/G39660.1

Gianardi, R., Bissona, M., Cocchic, L., Isaiad, R., Passaroe, S., Sepef, V., & Spinetti, C. (2024). From land to sea: A new high-resolution bathymetry and topography of the Campi Flegrei area, Southern Italy. *Journal of Maps*, *20*(1), 2404873. https://doi.org/10.1080/17445647.2024.2404873

Goswami, R., Mitchell, N. C., Brocklehurst, S. H., & Argnani, A. (2017). Linking subaerial erosion with submarine geomorphology in the western Ionian Sea (south of the Messina Strait), Italy. *Basin Research*, *29*, 641–658. https://doi.org/10.1111/bre.12196

Guida, D., & Valente, A. (2019). Terrestrial and marine landforms along the Cilento coastland (southern Italy): A framework for landslide hazard assessment and environmental conservation. *Water*, *11*(12), 2618. https://doi.org/10.3390/w11122618

Harff, J., Bailey, G., & Luth, F. (2016). Geology and archaeology: Submerged landscapes of the continental shelf: An introduction. *Geological Society, London, Special Publications*, *411*, 1–8. https://doi.org/10.1144/SP411.13

Jegen, M., Haroon, A., Schwalenberg, K., Müller, T. H., Schmidt, M., Pandolpho, B., Giona Bucci, M., Hrozal, S., & Sakellariou, D. (2024). Gulf of Corinth groundwater-is the deep offshore freshened, groundwater body within the Gulf of Corinth actively recharging? Cruise No. M196, 5.12. 2023-27.12. 2023, Piraeus (Greece) – Limassol (Cyprus). GoCW. METEOR-Berichte, M196. Begutachterpanel Forschungsschiffe, Bonn, 92. https://doi.org/10.48433/cr_m196.

Karymbalis, E., Ferentinou, M., & Giles, P. T. (2018). Use of morphometric variables and self-organizing maps to identify clusters of alluvial fans and catchments in the north Peloponnese, Greece. *Geological Society, London, Special Publications*, *440*(1), 45–64. https://doi.org/10.1144/SP440.7

Karymbalis, E., Gaki-Papanastassiou, K., Tsanakas, K., & Ferentinou, M. (2016a). Geomorphology of the Pinios River delta, Central Greece. *Journal of Maps*, *12*(1), 12–21. https://doi.org/10.1080/17445647.2016.1153356

Karymbalis, E., Papanastassiou, D., Gaki-Papanastassiou, K., Ferentinou, M., & Chalkias, C. (2016b). Late Quaternary rates of stream incision in Northeast Peloponnese, Greece. *Frontiers of Earth Sciences*, *10*(3), 455–478. https://doi.org/10.1007/s11707-016-0577-0

Karymbalis, E., Papanastassiou, D., Gaki-Papanastassiou, K., Tsanakas, K., & Maroukian, H. (2013). Geomorphological study of Cephalonia Island, Ionian Sea, Western Greece. *Journal of Maps*, *9*(1), 121–134. https://doi.org/10.1080/17445647.2012.758423

Kershaw, S., & Guo, L. (2001). Marine notches in coastal cliffs: Indicators of relative sea-level change, Perachora Peninsula, central Greece. *Marine Geology*, *179*(3), 213–228. https://doi.org/10.1016/S0025-3227(01)00218-3

Koukis, G., Sabatakakis, N., Ferentinou, M., Lainas, S., Alexiadou, X., & Panagopoulos, A. (2009). Landslide phenomena related to major fault tectonics: Rift zone of Corinth Gulf, Greece. *Bulletin of Engineering Geology and the Environment*, *68*(2), 215–229. https://doi.org/10.1007/s10064-008-0184-8

Leeder, M. R., Mc Neill, L. C., Collier, R. E., Portman, C., Rowe, P. J., Andrews, J. E., & Gawthorpe, R. L. (2003). Corinth rift margin uplift: New evidence from Late Quaternary marine shorelines. *Geophysical Research Letters*, *30*(12), 1611. https://doi.org/10.1029/2003GL017382

Leeder, M. R., Seger, M., & Stark, C. P. (1991). Sedimentation and tectonic geomorphology adjacent to major active and inactive normal faults, southern Greece. *Journal of the Geological Society*, *148*(2), 331–343. https://doi.org/10.1144/gsjgs.148.2.0331

Maroukian, H., Gaki-Papanastassiou, K., Karymbalis, E., Vouvalidis, K., Pavlopoulos, K., Papanastassiou, D., & Albanakis, K. (2008). Morphotectonic control on drainage network evolution in the Perachora peninsula, Greece. *Geomorphology*, *102*(1), 81–92. https://doi.org/10.1016/j.geomorph.2007.07.021

Mattei, G., Troisi, S., Aucelli, P., Pappone, G., Peluso, F., & Stefanile, M. (2018). Sensing the submerged landscape of Nisida Roman Harbour in the Gulf of Naples from integrated measurements on a USV. *Water*, *10*(11), 1686. https://doi.org/10.3390/w10111686

Mayer, L., Jakobsson, M., Allen, G., Dorschel, B., Falconer, R., Ferrini, V., Lamarche, G., Snaith, H., & Weatherall, P. (2018). The Nippon Foundation – GEBCO Seabed 2030 Project: The Quest to See the World's Oceans Completely Mapped by 2030. *Geosciences*, *8*(2), 63. https://doi.org/10.3390/geosciences8020063

Miccadei, E., Orrù, P., Piacentini, T., Mascioli, F., & Puliga, G. (2012). Geomorphological map of the Tremiti Islands (Puglia, Southern Adriatic Sea, Italy), scale 1:15,000.

Journal of Maps, *8*(1), 74–87. https://doi.org/10.1080/17445647.2012.668765

Mondillo, N., Di Nuzzo, M., & Balassone, G. (2022). Petrographic and geochemical features of the B3 bauxite horizon (Cenomanian-Turonian) in the Parnassos-Ghiona area: A contribution towards the genesis of the Greek karst bauxites. *Ore Geology Reviews*, *143*(4), 104759. https://doi.org/10.1016/j.oregeorev.2022.104759

Nixon, C. W., McNeill, L. C., Gawthorpe, R. L., Shillington, D. J., Michas, G., Bell, R. E., Moyle, A., Ford, M., Zakharova, N. V., Bull, J. M., & de Gelder, G. (2024). Increasing fault slip rates within the Corinth Rift, Greece: A rapidly localising active rift fault network. *Earth and Planetary Science Letters*, *636*, 118716. https://doi.org/10.1016/j.epsl.2024.118716

Nomikou, P., Alexandri, M., Lykousis, V., Sakellariou, D., & Ballas, D. (2011). Swath bathymetry and morphological slope analysis of the Corinth Gulf. *Proceedings of the 2nd INQUA-IGCP-567 International Workshop on Active Tectonics, Earthquake Geology, Archaeology and Engineering* (pp. 155–158).

Ori, G. G. (1989). Geologic history of the extensional basin of the Gulf of Corinth (?Miocene-Pleistocene), Greece. *Geology*, *17*(10), 918–921. https://doi.org/10.1130/0091-7613(1989)017 < 0918:GHOTEB>2.3.CO;2

Orrù, E. P., Demurtas, V., Meleddu, A., Paliaga, E., Todde, S., & Deiana, G. (2024). Geohazard features of the Southern Sardinia. *Journal of Maps*, *20*(1), 2375093. https://doi.org/10.1080/17445647.2024.2375093

Papadopoulou-Vrynioti, K., & Bellos, T. (2001). Geomorphological observations in karst landforms in the mountains of Parnassos – Helikon – Giona. *Bulletin of the Geological Society of Greece*, *34*(1), 439–442. https://doi.org/10.12681/bgsg.17047

Papanikolaou, D. J., & Royden, L. H. (2007). Disruption of the Hellenic arc: Late Miocene extensional detachment faults and steep Pliocene-Quaternary normal faults – or what happened at Corinth?. *Tectonics*, *26*(5), TC5003. https://doi.org/10.1029/2006TC002007

Parrott, D. R., Todd, B. J., Shaw, J., Hughes Clarke, J. E., Griffin, J., MacGowan, B., Lamplugh, M., & Webster, T. (2008). Integration of multibeam bathymetry and LiDAR surveys of the Bay of Fundy, Canada. *Proceedings of the Canadian Hydrographic Conference and National Surveyors Conference 2008* (p. 15).

Pirazzoli, P. A., Stiros, S. C., Arnold, M., Laborel, J., Laborel-Deguen, F., & Papageorgiou, S. (1994). Episodic uplift deduced from Holocene shorelines in the Perachora Peninsula Corinth area, Greece. *Tectonophysics*, *229*(3-4), 201–209. https://doi.org/10.1016/0040-1951(94)90029-9

Prampolini, M., Foglini, F., Biolchi, S., Devoto, S., Angelini, S., & Soldati, M. (2017). Geomorphological mapping of terrestrial and marine areas, northern Malta and Comino (central Mediterranean Sea). *Journal of Maps*, *13*(2), 457–469. https://doi.org/10.1080/17445647.2017.1327507

Prampolini, M., Gauci, C., Micallef, A. S., Selmi, L., Vandelli, V., & Soldati, M. (2018). Geomorphology of the north-eastern coast of Gozo (Malta, Mediterranean Sea). *Journal of Maps*, *14*(2), 402–410. https://doi.org/10.1080/17445647.2018.1480977

Prampolini, M., Savini, A., Foglini, F., & Soldati, M. (2020). Seven good reasons for integrating terrestrial and marine datasets in changing environments. *Water*, *12*(8), 2221. https://doi.org/10.3390/w12082221

Reilinger, R., McClusky, S., Paradissis, D., Ergintav, S., & Vernant, P. (2009). Geodetic constraints on the tectonic evolution of the Aegean region and strain accumulation along the Hellenic subduction zone. *Tectonophysics*, *488*(1-4), 22–30. https://doi.org/10.1016/j.tecto.2009.05.027

Roberts, G. P., Houghton, S. L., Underwood, C., Papanikolaou, I., Cowie, P. A., van Calsteren, P., Wigley, T., Cooper, F. J., & McArthur, J. M. (2009). Localization of Quaternary slip rates in an active rift in 10 5 years: An example from central Greece constrained by 234 U- 230 Th coral dates from uplifted paleoshorelines. *Journal of Geophysical Research*, *114*, B10406. https://doi.org/10.1029/2008JB005818

Sagawa, T., Yamashita, Y., Okumura, T., & Yamanokuchi, T. (2019). Satellite derived bathymetry using machine learning and multi-temporal satellite images. *Remote Sensing*, *11*(10), 1115. https://doi.org/10.3390/rs11101155

Sakellariou, D., & Galanidou, N. (2016). Pleistocene submerged landscapes and Palaeolithic archaeology in the tectonically active Aegean region. *Geological Society London Special Publications*, *411*, 145–178. https://doi.org/10.1144/SP411.9

Sakellariou, D., Lykousis, V., Alexandri, S., Kaberi, H., Rousakis, G., Nomikou, P., Georgiou, P., & Ballas, D. (2007). Faulting, seismic-stratigraphic architecture and Late Quaternary evolution of the Gulf of Alkyonides Basin–East Gulf of Corinth, Central Greece. *Basin Research*, *19*(2), 273–295. https://doi.org/10.1111/j.1365-2117.2007.00322.x

Sakellariou, D., Lykousis, V., & Rousakis, G. (2011). Holocene seafloor faulting in the Gulf of Corinth: The potential for underwater paleoseismology. *2nd INQUA-IGCP 567 International Workshop on Active Tectonics, Earthquake Geology, Archaeology and Engineering*. Proceedings (pp. 218–221).

Sakellariou, D., & Tsampouraki-Kraounaki, K. (2019). Plio-Quaternary extension and strike-slip tectonics in the aegean. In J. Duarte (Ed.), *Transform plate boundaries and fracture zones* (14, pp. 339–374). Elsevier. https://doi.org/10.1016/B978-0-12-812064-4.00014-1.

Sandwell, D. T., Gille, S. T., Orcutt, J., & Smith, W. H. (2003). Bathymetry from space is now possible. *Eos, Transactions American Geophysical Union*, *84*(5), 37–44.

Savini, A., Bracchi, V. A., Cammarosano, A., Pennetta, M., & Russo, F. (2021). Terraced landforms onshore and offshore the cilento promontory (South-Eastern Tyrrhenian Margin) and their significance as Quaternary records of sea level changes. *Water*, *13*(4), 566. https://doi.org/10.3390/w13040566

Seger, M., & Alexander, J. (2009). Distribution of plio-pleistocene and modern coarse-grained deltas south of the gulf of corinth, Greece. In L. E. Frostick (Ed.), *Tectonic controls and signatures in sedimentary successions* (pp. 37–48). John Wiley & Sons. https://doi.org/10.1002/9781444304053.ch3.

Soldati, M., Prampolini, M., Foglini, F., & Savini, A. (2021). Landscapes and landforms of terrestrial and marine areas: A way forward. *Water*, *13*(9), 1201. https://doi.org/10.3390/w13091201

Stefatos, A., Papatheodorou, G., Ferentinos, G., Leeder, M., & Collier, R. (2002). Seismic reflection imaging of active offshore faults in the Gulf of Corinth: Their seismotectonic significance. *Basin Research*, *14*(4), 487–502. https://doi.org/10.1046/j.1365-2117.2002.00176.x

Susa, T. (2022). Satellite derived bathymetry with sentinel-2 imagery: Comparing traditional techniques with

advanced methods and machine learning ensemble models. *Marine Geodesy*, *45*(5), 435–461. https://doi.org/10.1080/01490419.2022.2064572

Taddia, Y., Stecchi, F., & Pellegrinelli, A. (2020). Coastal Mapping Using DJI Phantom 4 RTK in Post-Processing Kinematic Mode. *Drones*, *4*(2), 9. https://doi.org/10.3390/drones4020009

Tang, K. K. W., & Mahmud, M. R. (2021). The accuracy of satellite derived bathymetry in Coastal and Shallow Water Zone. *International Journal of Built Environment and Sustainability*, *8*(3), 1–8. https://doi.org/10.11113/ijbes.v8.n3.681

Terefenko, P., Zelaya Wziątek, D., Dalyot, S., Boski, T., & Pinheiro Lima-Filho, F. (2018). A high-precision LiDAR-based method for surveying and classifying coastal notches. *ISPRS International Journal of Geo-Information*, *7*(8), 295. https://doi.org/10.3390/ijgi7080295

Tiede, J., Jordan, C., Moghimi, A., & Schlurmann, T. (2023). Long-term shoreline changes at large spatial scales at the Baltic Sea: Remote-sensing based assessment and potential drivers. *Frontiers in Marine Science*, *10*, 1207524. https://doi.org/10.3389/fmars.2023.1207524.

Tsakanikou, P., Galanidou, N., & Sakellariou, D. (2021). Lower Palaeolithic archaeology and submerged landscapes in Greece: The current state of the art. *Quaternary International*, *584*, 171–181. https://doi.org/10.1016/j.quaint.2020.05.025.

Tsanakas, K., Karymbalis, E., Gaki-Papanastassiou, K., & Maroukian, H. (2019). Geomorphology of the Pieria Mtns, Northen Greece. *Journal of Maps*, *15*(2), 499–508. https://doi.org/10.1080/17445647.2019.1619630.

Tsanakas, K., Karymbalis, E., Griva, D., Valkanou, K., Batzakis, D. V., Vassilakis, E., Konsolaki, A., & Gaki-Papanasassiou, K. (2025). The geomorphology of Greece. *Journal of Maps*, *21*(1), 2540555. https://doi.org/10.1080/17445647.2025.2540555

Tzvetkov, J. (2018). Relief visualization techniques using free and open source GIS tools. *Polish Cartographical Review*, *50*(2), 61–71. https://doi.org/10.2478/pcr-2018-0004

Vandelli, V., Sarkar, N., Micallef, A. S., Soldati, M., & Rizzo, A. (2023). Coastal inundation scenarios in the north-eastern sector of the Island of Gozo (Malta, Mediterranean Sea) as a response to sea level rise. *Journal of Maps*, *19*(1), 2145918. https://doi.org/10.1080/17445647.2022.2145918

Wölfl, A. C., Snaith, H., Amirebrahimi, S., Devey, C. W., Dorschel, B., Ferrini, V., Huvenne, V. A. I., Jakobsson, M., Jencks, J., Johnston, G., Lamarche, G., Mayer, L., Millar, D., Pedersen, T. H., Picard, K., Reitz, A., Schmitt, T., Visbeck, M., Weatherall, P., & Wigley, R. (2019). Seafloor mapping – the challenge of a truly global ocean bathymetry. *Frontiers in Marine Science*, *6*, 238. https://doi.org/10.3389/fmars.2019.00283

Yokoyama, R., Shirasawa, M., & Pike, R. J. (2002). Visualizing topography by openness. A new application of image processing to DEMs. *Photogrammetric Engineering and Remote Sensing*, *68*(3), 257–265.

Terrestrial and submarine geomorphological map of the Gulf of Corinth and surrounding areas, Greece

Sofia ROSSI[1,2], Konstantinos TSANAKAS[3], Monica GIONA BUCCI[4,5], Dimitris SAKELLARIOU[6], Mauro SOLDATI[1], Efthimios KARYMBALIS[3]

[1]Department of Chemical and Geological Sciences, University of Modena and Reggio Emilia, Italy
[2]School of Advanced Studies (IUSS) of Pavia, Italy
[3]Department of Geography, Harokopio University of Athens, Greece
[4]Marine Geology and Seafloor Surveying Group, University of Malta, Malta
[5]R3Vox, Mdina Road, Central Business District, Malta
[6]Institute of Oceanography, Hellenic Centre for Marine Research, Greece

Corresponding author: sofia.rossi@unimore.it

0 10 20 30 km

1:150,000

Coordinate System: Greek Geodetic Reference System 1987 (HGRS87)

N

Geodynamic setting

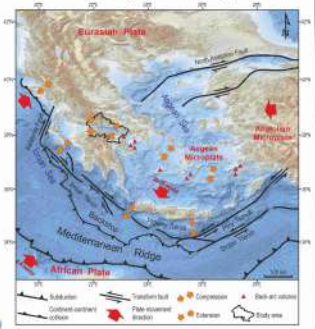

LEGEND

Bedrock
- Conglomerates
- Marls, sandstones, and clays
- Flysch
- Siliceous sedimentary rocks
- Carbonate sedimentary rocks
- Igneous rocks
- Metamorphic rocks
- Bauxite
- Submerged bedrock

Structural elements and landforms
- Edge of structural scarp
- Edge of submerged structural scarp
- Normal fault
- Mostly active normal fault
- Knickpoint

Coastal elements and landforms
- Present-day coastline
- Uplifted marine terrace surface
- Perched Gilbert delta topsets (Middle-Late Pleistocene)
- Perched Gilbert delta topsets (Calabrian)
- Emerged tidal notch
- Submerged tidal notch

Marine elements and landforms
- Submarine sediments
- Submerged fan
- Sediment wave
- Cyclic steps
- Pockmark
- Depression within contourites
- Edge of submerged erosional scarp
- Submerged channel
- Submerged single channel canyon valley
- Submerged single channel canyon
- Submerged gully

Gravity-induced landforms
- Talus and scree
- Debris flow fan
- Landslide scarp
- Submerged landslide scarp
- Landslide deposit
- Submerged landslide deposits
- Slip surface area of submarine landslide
- Submerged debris flow heaps

Karst landforms
- Polje
- Hum
- Solution doline
- Collapse doline
- Doline field
- Cave entrance

Fluvial landforms
- Alluvial plain
- Alluvial fan
- Alluvial and debris flow fan
- Channel deposits
- Terrace surface
- Badlands
- Edge of fluvial scarp
- Gorge
- Crest
- Palaeo-flow direction

Glacial landforms
- Glacial deposits

Geomorphological cross-section